



Characterizing and predicting smoldering temperature variations based on non-linear mixed effects models

Sainan Yin^{1,2} · Yanlong Shan^{1,2} · Bo Gao^{1,2} ·
Shuyuan Tang^{1,2} · Xiyue Han^{1,2} · Guojiang Zhang^{1,2} ·
Bo Yu^{1,2} · Shan Guan^{1,2}

Received: 16 November 2021 / Accepted: 20 December 2021 / Published online: 19 March 2022
© Northeast Forestry University 2022

Abstract Underground fires are slow spreading, long-lasting and low temperature smoldering combustion without flames, mainly occurring in peatlands and wetlands with rich organic matter. The spread of the smoldering is maintained by heat released during combustion and monitoring this is an important approach to detect underground fires. The Daxing'an Mountains region is a hotspot for underground fires in northeast China. This study examined a *Larix gmelinii* plantation in the Tatou wetlands of the Daxing'an Mountains and determined the maximum temperature variation of humus of varying particle sizes, and the temperature rising process based on non-linear mixed effects models by an indoor combustion experiment. Maximum combustion temperatures up to 897.5 °C, increased with humus depth; among the three models tested, Richard's equations were best for characterizing temperature variations; a non-linear equation with three parameters had the highest accuracy in fitting the combustion temperature variations with varying humus particle sizes. These results are informative for

predicting temperature variations and provide technical support for underground fire monitoring.

Keywords Underground fire · NLME modeling · Smoldering temperature · Daxing'an mountains

Introduction

Forest fires are classified into surface, canopy, and underground fires. Underground fires occur less frequently than the other types, but the damage can be significant (Watts and Kobziar 2013). Underground forest fire is slow spreading, long-lasting and having low temperature smoldering combustion without flame (Ohlemiller 1985; Rein 2013). These fires cause fatal damage to plant roots (Page et al. 2002; Davies et al. 2013), destruction of soil structure and ground collapse (Hadden et al. 2013), and higher greenhouse gas emissions than other categories of forest fires (Turetsky et al. 2004). Forested peatlands and wetlands with rich organic matter, such as those in boreal and tropical forests, are prone to underground fire (Huang et al. 2016). Soil carbon in these forests accounts for 25% of carbon reserves on land and plays essential roles in ecosystem stability, biodiversity maintenance, and hydrological cycling (Page et al. 2011). Therefore, large underground fires will substantially impact global climate, ecology, and human health (Davies et al. 2013; Hu et al. 2018). Wetlands were previously assumed to be fire-resistant due to their high humidity (Kuhry 1994). However, recent studies reported that smoldering has been widely observed in wetlands (Turetsky et al. 2004; Shetler et al. 2008). Quantitative studies in the field on smoldering events are seldom conducted as they are challenging due to their randomness and unpredictability (Davies et al. 2013).

Project funding: This research was funded by the National Natural Science Foundation of China (Grant No. 31971669).

The online version is available at <http://www.springerlink.com>

Corresponding editor: Yu Lei

✉ Yanlong Shan
shanyl@163.com

- ¹ Science and Technology Innovation Center of Wildland Fire Prevention and Control, Beihua University, 3999 Binjiang East Road, Jilin City 132013, Jilin, People's Republic of China
- ² Forestry College, Beihua University, 3999 Binjiang East Road, Jilin City 132013, Jilin, People's Republic of China

Therefore, combustion studies simulating underground fires are often carried out in the laboratory (Huang et al. 2015).

Large-scale underground fires have been recorded in Indonesia, Russia, Spain, and in other countries in recent years (Page et al. 2002; Cancellieri et al. 2012; Turetsky et al. 2015; Pastor et al. 2018). Underground fires are caused by surface fires or lightning (Davies 2016; Restuccia et al. 2017) with strong concealment and always accompanied by surface fires. There are considerable difficulties in monitoring and extinguishing them (Rein et al. 2008a, b). Their behavior is significantly different from other types of fires (Rein 2013), and could occur with a fuel moisture content of 100% or higher (Reardon et al. 2007; Lin et al. 2019), and persist through heavy rains, weather changes, extinguishing of surface fires, and may last for months or even years (Zaccone et al. 2014). The spread of an underground fire is maintained by heat released during combustion (Pastor et al. 2018), which is key to monitoring (Hartford and Frandsen 1992). Studies of smoldering have mainly focused on combustion characteristics (Pastor et al. 2018), contributing factors (Achte-meier 2006; Wang et al. 2017), combustion spread (Huang and Rein 2017), carbon release (Davies et al. 2013; Hu et al. 2018) and other aspects.

Non-linear mixed effects (NLME) modeling was first proposed by Sheiner and Beal (1980), which included both fixed and random effects parameters, and could identify average prediction and individual prediction by calculating the estimated value of random effect parameters (Leites and Robinson 2004; Dorado et al. 2006; Yang et al. 2009). A mixed-effects model is a statistical method used in forestry, agriculture, ecology, biomedicine, sociology, economics, and in other fields (Calegario et al. 2005). In forestry, NLME modeling has been used in the studies of tree heights and diameters, growth processes, average growth, and basal area (Budhathoki et al. 2008; Mehtatalo et al. 2014; Ciceu et al. 2020) but has been seldom applied to forest fires. The mechanism of underground fire smoldering is complicated, so its occurrence and development are difficult to predict. The gradually rising temperature of a smoldering fire is like the growth process of a tree, so NLME modeling is applicable to smoldering. NLME modeling can achieve prediction accuracy with fewer independent variables and is suitable for studies on underground fire.

The frequency of underground fires in the boreal forests has increased in recent years (Sinclair et al. 2020), due to global climate change and the impact of human activities (Turetsky et al. 2015). The coniferous forests in the Daxing'an Mountains region, the southernmost margin of the Far Eastern Siberia boreal forests into China, is characterized by the largest number of underground fires in the country. The growth of *Larix gmelinii* (Rupr.) Rupr. planted in the Tatou wetlands of the Daxing'an Mountains has been poor because of the geographical and climatic conditions,

and the decomposition of fallen branches and leaves slow so that the content of organic matter in humus increased, providing abundant fuel for underground fires. Rising temperature is one of the stages during the smoldering (Pastor et al. 2018); one of these is the buildup of temperatures causing significant damages. However, this process is easily monitored. This study focused on the process of rising temperatures in a *Larix gmelinii* plantation in the Tatou wetlands, analyzed smoldering temperature variations of humus of different particle sizes, and developed a method to predict temperatures of underground fires by non-linear mixed effects (NLME) modeling to provide support for underground fire monitoring and control.

Materials and methods

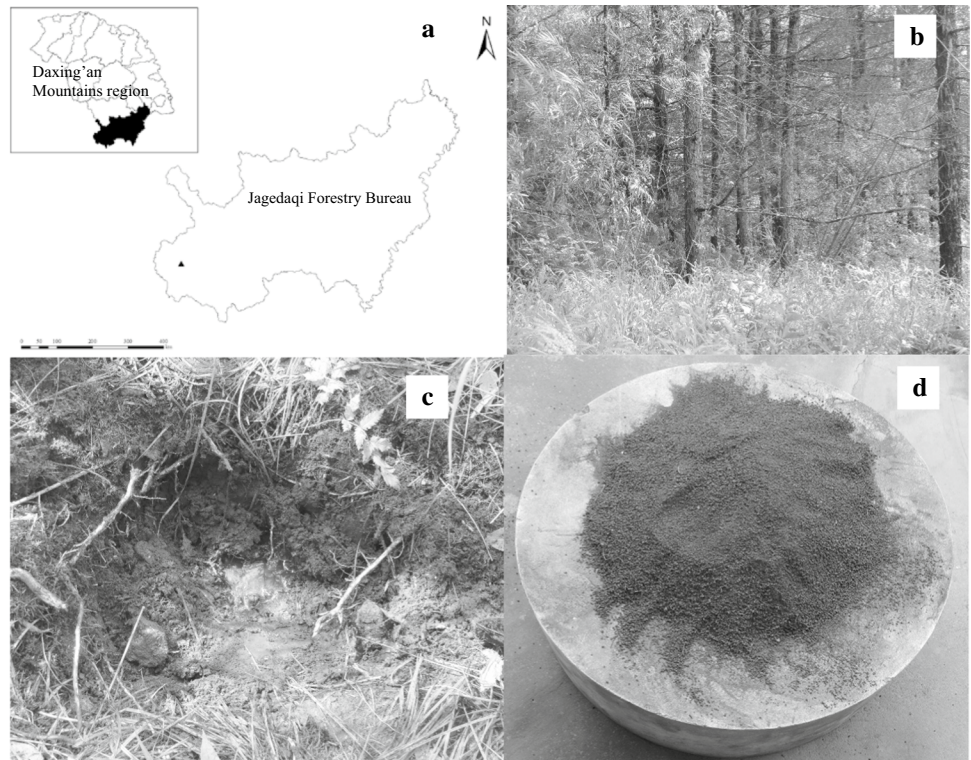
Study area

Forest fires in the Daxing'an Mountains region occur frequently; the area burned is largest in China. The study area is in the Jiagedaqi Forest Management Technology Promotion Station (123°57'–124°0' E, 50°20'–50°23' N), located in the northwest of Heilongjiang province, on the southeast slopes of the Daxing'an Mountains (Fig. 1a). The region has a continental monsoon climate with four distinctive seasons, a changeable climate and large diurnal and seasonal temperature differences. Annual average temperatures are –1 to 2 °C, the annual effective accumulative temperature 1800–2000 °C, the frost-free period 90–120 days, and annual rainfall 450–500 mm. The technology promotion station was founded in 1973, 15 km to the south of the Jiagedaqi region, the north and west portions of the station is connected with the Dongfeng Forest Station of the Jiagedaqi Forestry Bureau. The total area of the station is 7326 ha². The main species in the study area are *Larix gmelinii*, *Quercus mongolica* Fisch., *Betula platyphylla* Suk., *Populus davidiana* Dode, and *Betula dahurica* Pallas (Tang et al. 2022).

Sample collection and processing

Three 30 m × 20 m sample fields were established and three 0.5 cm × 0.5 cm quadrats selected (sampling depth was the 46-cm thickness of the humus layer) in the diagonals according to Pastor (2018) (Fig. 1b, c). All the humus in the quadrats was collected, and after removal of surface litter and in the humus layer, taken to the laboratory, stored in kraft paper sacks and dried for 48 h at 105 °C to remove as much moisture as possible. As an uneven distribution of humus particles will affect the temperature measurements accuracy (Huang and Rein 2017), the dried humus was ground and sieved into particle sizes

Fig. 1 **a** The study area; **b**, **c** study location and sample collection; **d** sample after pretreatment for the combustion experiment



of ≤ 20 mesh (moisture content 0.28%), ≤ 40 mesh (moisture content 0.49%), ≤ 60 mesh (moisture content 0.43%), and ≤ 80 mesh (moisture content 0.49%) for the combustion experiments (Fig. 1d).

Combustion experiments

The combustion furnace was designed for studying a one-dimensional downward combustion process (Fig. 2) (Huang

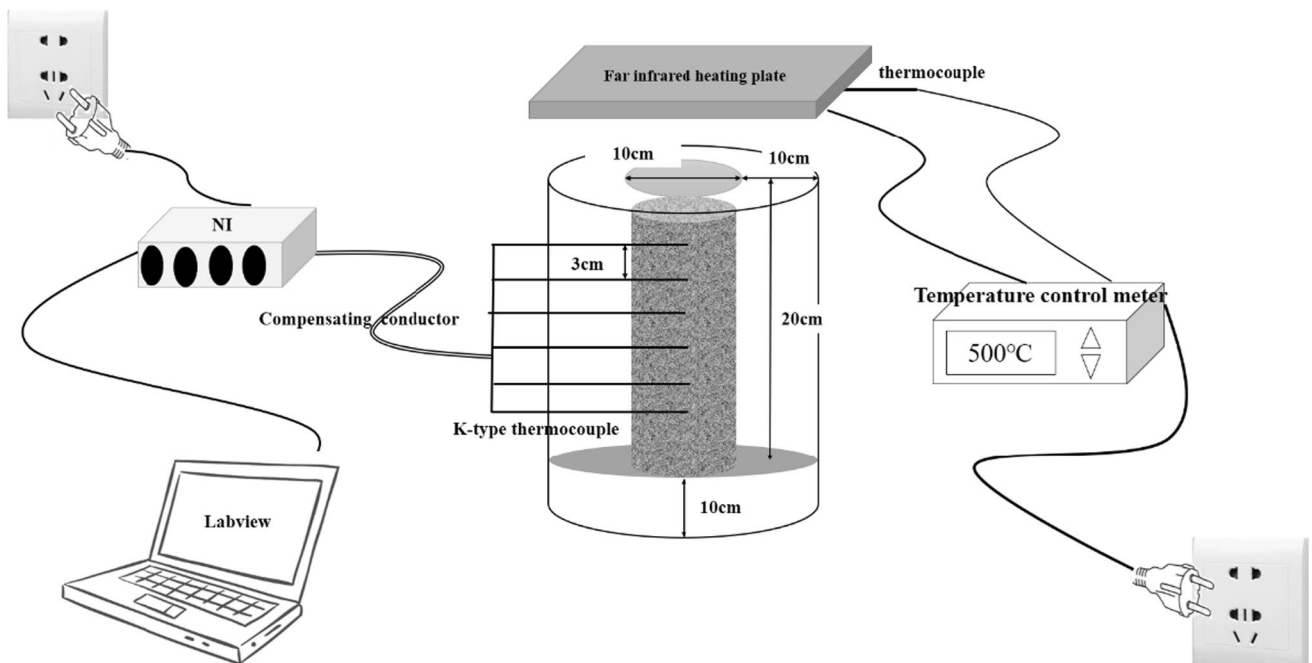


Fig. 2 Schematic diagram of the smoldering combustion process

and Rein 2017). The unit was cylindrical (20- cm high with 10- cm walls) of aluminum silicate ceramic fiber with excellent heat insulation. A K-type thermocouple (30 cm long×2 mm diameter) recorded temperature variations of the humus during combustion. The data were transmitted to a laptop by data acquisition module composed of a 16-channel NI9213 voltage acquisition board card and DAQ-9174 case (4 card slots), with temperature measurement accuracy <0.25 °C. The data acquisition software (Labview2018) recorded temperature variations collected by the thermocouples. A far-infrared heating plate (30 cm long×20 cm wide×5 cm thick) was used as an ignition device. A temperature control meter between the far-infrared heating plate and the power supply kept the temperature of the heating plate constant.

Humus of different particle sizes were placed in the combustion furnace at ambient temperatures and the shape of the particles maintained as much as possible. Holes were arranged every 3 cm on the side of combustion furnace and K-type thermocouples inserted into the humus through the holes. The K-type thermocouples and data acquisition module were connected temperature variation data transmitted to the laptop every 10 s. To ensure combustion continued after removing the heating plate (ignition device), heating time and temperature were set to 1.5 h and 500 °C. A 2-cm gap between the heating plate and combustion furnace allowed for air flow.

Non-linear mixed effects model

The general form of a non-linear mixed effects model is:

$$\begin{aligned}
 T_i &= f(\varphi_i, t_i) + \varepsilon_i \\
 \varphi_i &= A_i\beta + B_i b_i \\
 \varepsilon_i &\sim N(0, \sigma^2) \quad b_i \sim N(0, D)
 \end{aligned}
 \tag{1}$$

where T_i is the dependent variable of subject i and refers to the predicted combustion temperature; f is the actual value, specific parameter vector φ_i and variable value vector t_i of the differentiable function in the subject, and refers to actual combustion temperature of the underground fire; β is the p -dimensional fixed effect parameter vector; b_i is the q -dimensional random effect parameter vector; D is the covariance matrix between random effects; A_i and B_i are correlation

matrices with appropriate dimensions (0 or 1); t_i is the independent matrix; ε_i is the random error vector associated with T_i ; and, σ^2 is the covariance matrix of the random error.

Base model

Logistic, Richards, and Korf nonlinear models, widely used in forestry to predict the tree growth, height, and DBH (Calama and Montero 2004; Rijal 2012; Sharma et al. 2016; Pan et al. 2020) (Table 1), were selected as the base models to study temperature variations in the combustion process.

Model selection and validation

The base model was selected according to the values of Akaike’s Information Criterion-(AIC) and Schwarz’s Bayesian Information Criterion-(BIC). Model accuracy was evaluated with different parameters according to the values of Root Mean Square Error (RMSE). Smaller values of AIC and BIC indicate the better fitting degree of the equation; smaller values of RMSE indicates the higher accuracy of the model (Akaike 1974).

$$AIC = -2 \ln L + 2p \tag{2}$$

$$BIC = -2 \ln L + p \ln n \tag{3}$$

$$RMSE = \sqrt{\frac{\sum_{i=1}^n (T_{ij} - \hat{T}_{ij})^2}{n-1}} \tag{4}$$

where T_{ij} is the actual value, \hat{T}_{ij} the predicted value, n the sample amount, L the maximum likelihood (ML) value, and p is the number of model parameters.

Statistical analysis

Excel and Origin were used to analyze the combustion temperature variation data with different humus particle sizes and from different depths, and the relationship between the maximum temperature and the combustion depth; NLMIXED and NLIN modules of Statistical Analysis

Table 1 Base models

Model	Base model	Mixed-effects model
Logistic	$T_{ij} = \frac{\beta_1}{1 + \text{Exp}(\frac{\beta_2 - t_{ij}}{\beta_3})} + \varepsilon_{ij}$	$T_{ij} = \frac{(\beta_1 + b_{i,1})}{1 + \text{Exp}(\frac{(\beta_2 + b_{i,2}) - t_{ij}}{(\beta_3 + b_{i,3})})} + \varepsilon_{ij}$
Richards	$T_{ij} = \beta_1 [1 - \text{Exp}(-\beta_2 t_{ij})]^{\beta_3} + \varepsilon_{ij}$	$T_{ij} = (\beta_1 + b_{i,1}) [1 - \text{Exp}(-(\beta_2 + b_{i,2}) t_{ij})]^{\beta_3 + b_{i,3}} + \varepsilon_{ij}$
Korf	$T_{ij} = \beta_1 \text{Exp}(\frac{-\beta_2}{\beta_3}) + \varepsilon_{ij}$	$T_{ij} = (\beta_1 + b_{i,1}) \text{Exp}[\frac{-(\beta_2 + b_{i,2})}{t_{ij}(\beta_3 + b_{i,3})}] + \varepsilon_{ij}$

T_{ij} is temperature at depth j with time t of particle size i ; $\beta_1, \beta_2, \beta_3$ are the parameters of the equation; $b_{i,1}, b_{i,2}, b_{i,3}$ are random effect parameters corresponding to $\beta_1, \beta_2, \beta_3$; ε_{ij} is the random error

System-(SAS) were used to select, fit, and verify the non-linear mixed effect models.

Results

Maximum combustion temperature variations of humus of different particle sizes

There was no flame or spark during humus smoldering, and the surface was carbon black and the deep layer brick red after combustion. The maximum combustion temperature of different particle sizes increased with depth. There was a positive linear relationship between depth and temperature ($P < 0.05$) in both particle ≤ 40 mesh size and ≤ 80 mesh size. The equations were $y = 435.68 + 27.87x$ and $y = 453.82 + 21.82x$ respectively. The highest combustion temperature of all particle sizes was at the 15-cm depth with particles ≤ 40 mesh size (897.5 °C), the highest combustion temperature with particle ≤ 80 mesh size was 844.9 °C.

There was a positive linear relationship between depth and temperature ($P < 0.01$) in both particle ≤ 20 mesh size and ≤ 60 mesh size; the equations were $y = 474.76 + 17.42x$ and $y = 468.84 + 20.21x$, respectively. Combustion temperature variations with particle size ≤ 20 mesh at different depths fluctuated the lowest, the highest combustion temperature was 741.6 °C and the lowest was

543.3 °C. The highest combustion temperature with particle size ≤ 60 mesh was 780.4 °C and the lowest was 553.3 °C (Fig. 3).

Selection and validation of NLME models

The NLME models were selected based on 60% of the humus combustion data with different particle sizes. AIC, BIC evaluated the approximation based on the three models. The AIC (135,343) and BIC (135,373) values of the Richards equation with different particle sizes were the smallest. It may be concluded that Richards equation provided the best approximation and was therefore chosen as the basic equation for the relationship between humus combustion temperature and time (Table 2).

Richards equations of combustion temperature variation were set with no parameter mixing, and one, two, and three parameters mixing for different particle sizes. All equations with different parameters were convergent, and the RMSE values of models with mixed parameters were smaller than the traditional models. The precision of models with mixed parameters was higher than the conventional models. The RMSE value of the three parameters was the least, therefore, the accuracy of Richards equation with three parameters mixing was the highest (Table 3).

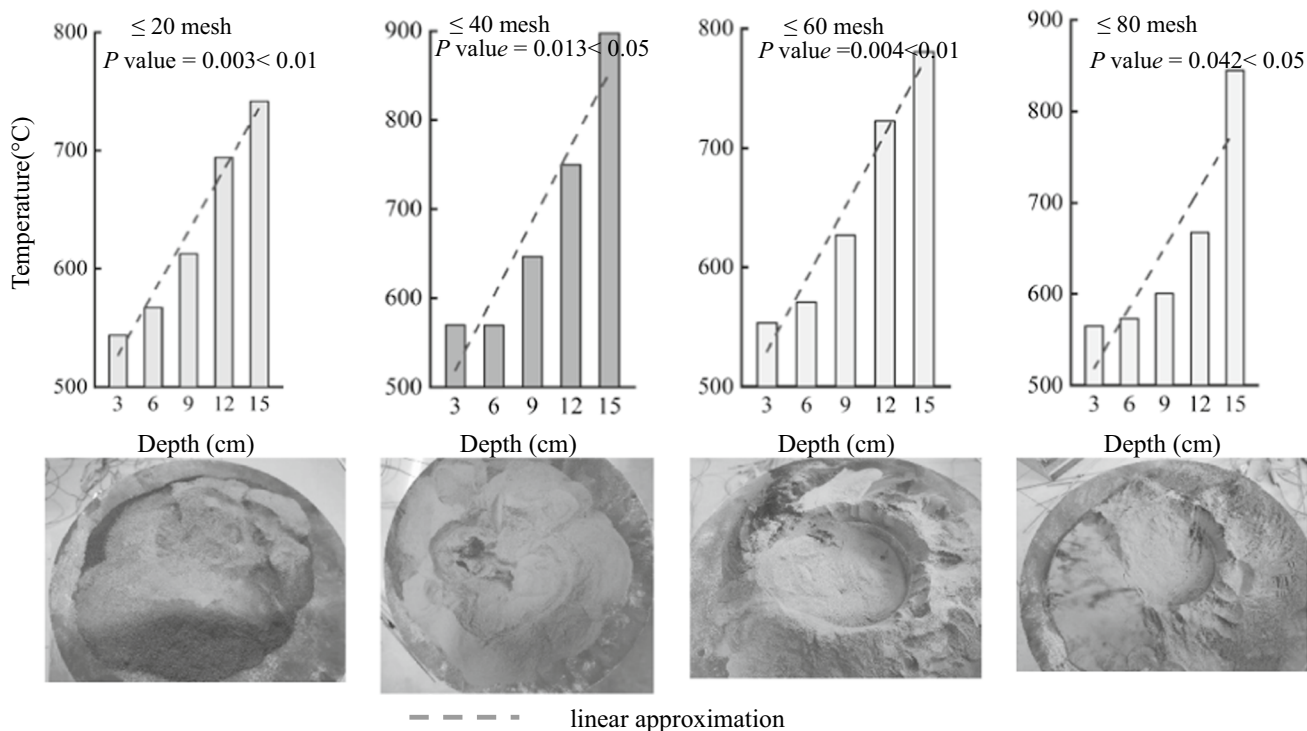


Fig. 3 Maximum combustion temperature of humus for different depths and particle sizes; lower panel are photos of humus after combustion

Table 2 Fit statistics

Particle size/mesh	Model	AIC	BIC
≤20	Logistic	136,412	136,442
	Richards	135,343	135,373
	Korf	135,435	135,465
≤40	Logistic	130,938	130,968
	Richards	129,637	129,666
	Korf	129,825	129,855
≤60	Logistic	143,822	143,851
	Richards	142,650	142,680
	Korf	142,774	142,804
≤80	Logistic	131,762	131,791
	Richards	131,430	131,459
	Korf	131,823	131,853

Mixed-effects model approximation of Richards equation

The relationship between combustion temperature and time at different depths with different particle sizes was fitted by Richards equation with three parameters mixing. According to the temperature variation, β_1, β_2 and β_3 were the estimated values of equations at 15- cm depth for each particle size, and b_{ij} was the parameter mixing effect at different depths (Table 4). The approximation of Richards equations with different particle sizes is shown in Fig. 4

Discussion and conclusions

Variation characteristics of humus combustion temperature

Peatland and humus are the main combustibles of underground fires, and peatland fires is of wide concern for the frequent occurrence of large-scale fires (Davies et al. 2013). Commercial peat moss with its homogenous texture and consistent components has been widely used in characterizing smoldering and contributing factors, instead of using peatlands in the field (Huang and Rein 2017). More researchers have started using underground combustibles to approximate reality (Pastor et al. 2018). In this study, actual humus from the Tatou wetlands of the Daxing’an Mountains was used to study temperature variations of vertical smoldering, and the results are reliable and highly applicable.

Smoldering combustion of humus is sustained by the heat released by itself. The maximum temperature was 897.5 °C in this study, close to 900 °C of a similar study using peat (Huang et al 2015). Most studies have reported that the maximum temperature of peat smoldering was around 600 °C (Bar-Ilan et al. 2004; Huang and Rein 2017), lower than

Table 3 Approximation results of mixed-effect models with different parameters

Particle size	Parameter	Mixed-effects	RMSE	P value
≤20 mesh	No parameter mixing	–	97.53	<0.001
	One parameter mixing	β_1	66.21	<0.001
		β_2	39.36	<0.001
		β_3	23.08	<0.001
	Two parameters mixing	$\beta_1 \beta_2$	19.63	<0.001
		$\beta_1 \beta_3$	19.91	<0.001
		$B_2 \beta_3$	20.38	<0.001
	Three parameters mixing	$\beta_1 \beta_2 \beta_3$	17.48	<0.001
	≤40 mesh	No parameter mixing	–	101.83
One parameter mixing		β_1	105.33	<0.001
		β_2	47.09	<0.001
		β_3	27.24	<0.001
Two parameters mixing		$\beta_1 \beta_2$	21.49	<0.001
		$\beta_1 \beta_3$	22.36	<0.001
		$B_2 \beta_3$	23.57	<0.001
Three parameters mixing		$\beta_1 \beta_2 \beta_3$	19.51	<0.001
≤60 mesh		No parameter mixing	–	94.43
	One parameter mixing	β_1	65.22	<0.001
		β_2	40.93	<0.001
		β_3	24.14	<0.001
	Two parameters mixing	$\beta_1 \beta_2$	24.25	<0.001
		$\beta_1 \beta_3$	20.14	<0.001
		$\beta_2 \beta_3$	20.77	<0.001
	Three parameters mixing	$\beta_1 \beta_2 \beta_3$	18.46	<0.001
	≤80 mesh	No parameter mixing	–	103.81
One parameter mixing		β_1	71.84	<0.001
		β_2	38.15	<0.001
		β_3	26.39	<0.001
Two parameters mixing		$\beta_1 \beta_2$	19.71	<0.001
		$\beta_1 \beta_3$	22.39	<0.001
		$\beta_2 \beta_3$	22.89	<0.001
Three parameters mixing		$\beta_1 \beta_2 \beta_3$	18.89	<0.001

our result. Using different experiment devices and materials might account for the difference. It could also reflect the different temperatures of humus and peat smoldering. The mass loss of combustibles was small, and the humus afterwards was brick red due to sufficient burning and high temperatures (Fig. 3) and in addition, there was no ash after combustion, only a thin layer of carbonized humus. The heat release was impeded by the humus of the upper layers when the fire was spreading downwards, so the temperature

Table 4 Fitting results of Richards equation

Particle size/mesh	Parameter	Estimate	Std error	Depth/cm	Approximate 95%	Confidence limits	Equation	
≤20	$b_{1,1}$	-223.50	2.72	3	-228.80	-218.20	$T = 574.3 \times [1 - \text{Exp}(-0.53 t)]^{1.05}$	
	$b_{2,1}$	0.40	0.01		0.38	0.41		
	$b_{3,1}$	-1.48	0.019		-1.52	-1.44		
	6	$b_{1,2}$	-207.40	2.44		-212.10	-202.60	$T = 590.4 \times [1 - \text{Exp}(-0.32 t)]^{1.25}$
		$b_{2,2}$	0.19	0.003		0.182	0.194	
		$b_{3,2}$	-1.28	0.0185		-1.32	-1.25	
	9	$b_{1,3}$	-158.2	2.40		-162.90	-153.50	$T = 639.6 \times [1 - \text{Exp}(-0.19 t)]^{1.44}$
		$b_{2,3}$	0.06	0.002		0.058	0.064	
		$b_{3,3}$	-1.09	0.0179		-1.13	-1.06	
	12	$b_{1,4}$	-18.40	3.03		-24.35	-12.45	$T = 779.4 \times [1 - \text{Exp}(-0.12 t)]^{1.68}$
		$b_{2,4}$	-0.014	0.001		-0.017	-0.012	
		$b_{3,4}$	-0.85	0.0181		-0.89	-0.82	
β_1		797.80	2.10	15	793.70	801.9		
β_2		0.13	0.0008		0.13	0.133		
β_3		2.53	0.02		2.50	2.56		
≤40	$b_{1,1}$	-304.4	3.3038	3	-310.80	-297.90	$T = 594.5 \times [1 - \text{Exp}(-0.50 t)]^{1.26}$	
	$b_{2,1}$	0.3617	0.00623		0.355	0.37		
	$b_{3,1}$	-1.5287	0.0234		-1.5746	-1.4829		
	6	$b_{1,2}$	-309.4	3.1742		-315.60	-303.10	$T = 589.5 \times [1 - \text{Exp}(-0.37 t)]^{1.44}$
		$b_{2,2}$	0.24	0.00385		0.23	0.25	
		$b_{3,2}$	-1.3514	0.0234		-1.3972	-1.3056	
	9	$b_{1,3}$	-225.1	3.1913		-231.30	-218.80	$T = 673.8 \times [1 - \text{Exp}(-0.21 t)]^{1.48}$
		$b_{2,3}$	0.0721	0.00184		0.0685	0.0757	
		$b_{3,3}$	-1.3134	0.0214		-1.3554	-1.2714	
	12	$b_{1,4}$	-76.2772	3.7035		-83.54	-69.02	$T = 822.6 \times [1 - \text{Exp}(-0.13 t)]^{1.92}$
		$b_{2,4}$	-0.00092	0.00134		-0.00354	-0.000171	
		$b_{3,4}$	-0.867	0.0223		-0.9107	-0.8233	
β_1		898.9	2.893	15	893.3	904.6		
β_2		0.1335	0.000919		0.1317	0.1353		
β_3		2.7887	0.0189		2.7518	2.8257		
≤60	$b_{1,1}$	-187.5	2.9790	3	-193.30	-181.60	$T = 606.3 \times [1 - \text{Exp}(-0.42 t)]^{0.99}$	
	$b_{2,1}$	0.2824	0.00698		0.2687	0.2961		
	$b_{3,1}$	-1.7329	0.0198		-1.7716	-1.6942		
	6	$b_{1,2}$	-196.0	2.1628		-200.20	-191.70	$T = 597.8 \times [1 - \text{Exp}(-0.29 t)]^{1.23}$
		$b_{2,2}$	0.1535	0.00295		0.1477	0.1593	
		$b_{3,2}$	-1.4939	0.0194		-1.5319	-1.4560	
	9	$b_{1,3}$	-132.1	2.1430		-136.30	-127.90	$T = 673.8 \times [1 - \text{Exp}(-0.21 t)]^{1.48}$
		$b_{2,3}$	0.0377	0.00151		0.0348	0.0407	
		$b_{3,3}$	-1.3198	0.0187		-1.3564	-1.2831	
	12	$b_{1,4}$	-2.0151	2.6009		-7.1129	-1.0827	$T = 822.6 \times [1 - \text{Exp}(-0.13 t)]^{1.92}$
		$b_{2,4}$	-0.0189	0.00112		-0.0211	-0.0167	
		$b_{3,4}$	-0.9724	0.0191		-1.0099	-0.9349	
15	β_1	793.8	1.7104		790.40	797.20	$T = 793.8 \times [1 - \text{Exp}(-0.14 t)]^{2.73}$	
	β_2	0.1381	0.000769		0.1366	0.1397		
	β_3	2.7252	0.0165		2.6929	2.7575		

Table 4 (continued)

Particle size/mesh	Parameter	Estimate	Std error	Depth/cm	Approximate 95%	Confidence limits	Equation
≤ 80	$b_{1,1}$	-274.8	3.5598	3	-281.80	-267.90	$T = 598.8 \times [1 - \text{Exp}(-0.51 t)]^{1.28}$
	$b_{2,1}$	0.4022	0.00657		0.3893	0.4151	
	$b_{3,1}$	-0.9529	0.0198		-0.9917	-0.9142	
	$b_{1,2}$	-278.1	3.3646	6	-284.70	-271.50	$T = 595.5 \times [1 - \text{Exp}(-0.36 t)]^{1.44}$
	$b_{2,2}$	0.2552	0.00359		0.2482	0.2623	
	$b_{3,2}$	-0.7887	0.0191		-0.8262	-0.7513	
	$b_{1,3}$	-251.5	3.2875	9	-257.90	-245.00	$T = 622.1 \times [1 - \text{Exp}(-0.22 t)]^{1.58}$
	$b_{2,3}$	0.1185	0.00182		0.1149	0.1220	
	$b_{3,3}$	-0.6517	0.0178		-0.6866	-0.6168	
	$b_{1,4}$	-129.3	3.6739	12	-136.50	-122.10	$T = 744.3 \times [1 - \text{Exp}(-0.12 t)]^{1.73}$
	$b_{2,4}$	0.0180	0.00120		0.0156	0.0203	
	$b_{3,4}$	-0.5026	0.0173		-0.5364	-0.4687	
	β_1	873.6	3.0904	15	867.6	879.7	$T = 873.6 \times [1 - \text{Exp}(-0.10 t)]^{2.23}$
	β_2	0.1040	0.000783		0.1024	0.1055	
	β_3	2.2323	0.0138		2.2053	2.2592	

of humus smoldering was higher and increased with depth. But the mass loss of combustibles in peat smoldering was larger according to Huang and Rein (2014). Without being impeded by upper layers, the heat released quickly so the temperature was lower than the humus.

Combustion depth could go to more than 50 cm (Ballhom et al. 2009). However, the combustion depth was found to be deeper due to the increased aridity of peatlands and wetlands due to global warming (Turetsky et al. 2015). The combustion process is also affected by oxygen levels, so when oxygen decreases as depth increases, combustion might be extinguished. This observation requires further study.

Applicability of NLME in smoldering temperature variation

Unlike surface and canopy fires, the heat released in underground fires is the manifestation of the smoldering process, which is also the important basis for fire monitoring and fighting. Fire intensity and spread rate are both predicted by the heat released (Rein et al. 2008a, b; Kirschke et al. 2013); the heat released, and temperature change of the ground surface are useful for judging the occurrence of underground fires and the direction for digging fire breaks. Therefore, thermos physical models are essential tools for studying the mechanism of underground fire occurrence and development (Huang and Rein 2014), and an important basis for fire monitoring and fighting.

This study was based on NLME modeling to predict temperatures of underground fires and focused on the prediction of temperature during smoldering. Simple statistical models are better for prediction research, and NLME is better than ordinary regression models. Many statistical models have been applied to forest fire prediction (Bem et al. 2018; Nadeem et al. 2020) and have increased prediction accuracy. The variation of temperatures during underground fire combustion showed a slow rise at the beginning, then a rapid rise, and finally, a stable temperature after reaching the maximum temperature. The change curves of the three basic models in this paper are "S" type, which are consistent with the change curves of underground fires, so the models could be applied to the prediction of temperatures during these fires.

In this study, well-replicated underground fire temperatures with varying depths and particle sizes were studied (Hall and Bailey 2001). NLME modeling was shown to be significantly superior in handling longitudinal, multi-level and replicated data (Calegario et al. 2005). Richards equations exhibited the best applicability in fitting humus combustion temperatures after evaluating three models and have been widely used owing to their biological significance, strong adaptability, and high accuracy (Li and Zhang 2010). Hang et al. (1997) and Hall and Bailey (2001) also found high accuracy of Richards equations, consistent with the results of our study.

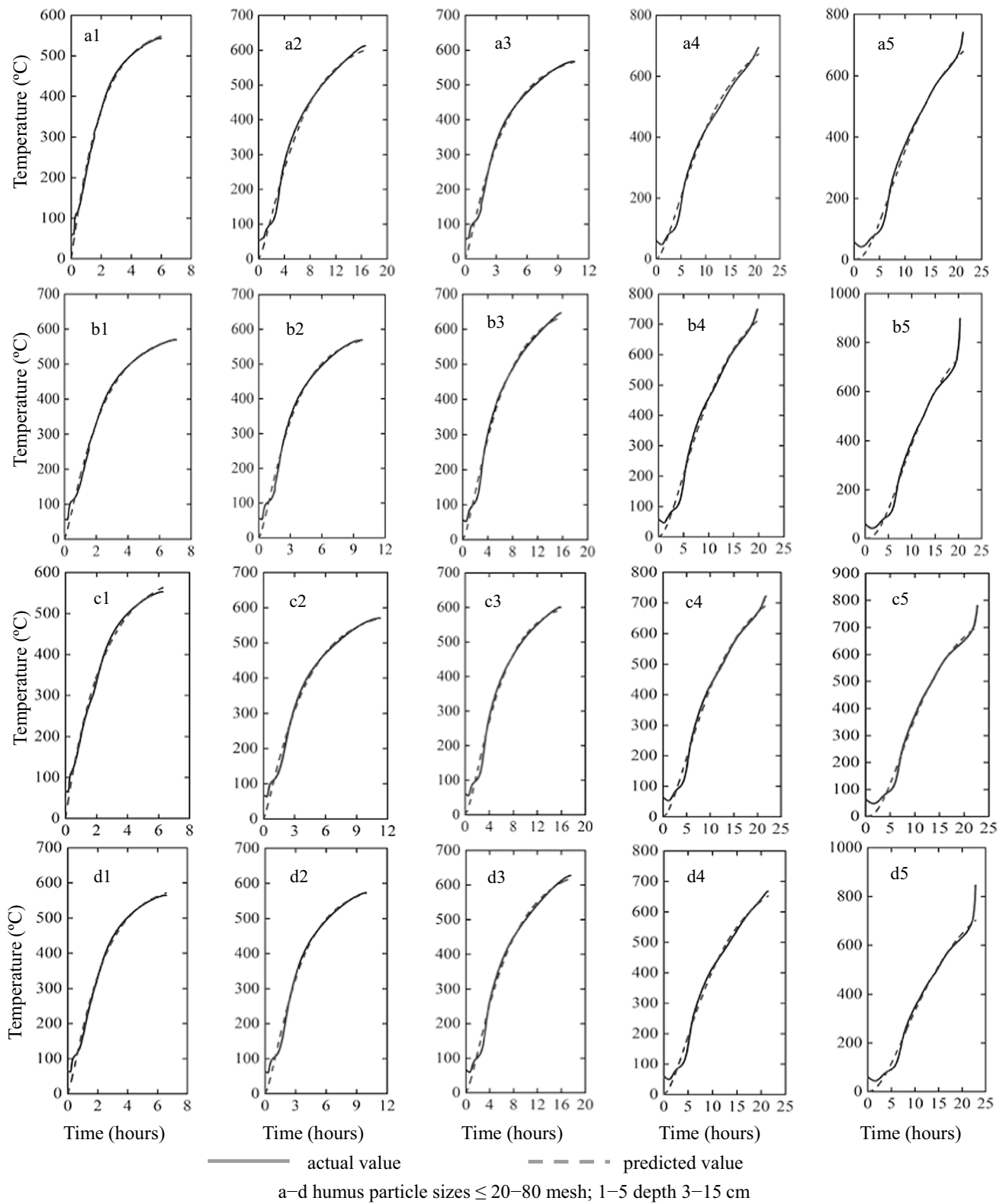


Fig. 4 Approximation of Richards equations of temperature and time at different depths with different humus particle sizes

Conventionally, the least square method was used to estimate model parameters of multilevel data, but this method tended to use data lacking independence, time correlation and space heterogeneity, and would lead to large prediction errors (Mensah et al. 2018). NLME modeling has higher accuracy (Sharma et al. 2016) through set up, fixed effect, and random effect parameters (Kalle 2009). Based on the results of RMSE in this study, the accuracy of models with mixing parameters were much higher than traditional nonlinear models, and the accuracy increased as the number of parameters increased. Ciceu et al. (2020) also reported the high precision of NLME models, although the parameters were different due to the research contents and basic models. Meng et al. (2009) found that a NLME model with two parameters was highly accurate. Pan et al. (2020) reported that one with three parameters had high precision.

Prospect of using NLME modeling in forest fire research

Studies with mixed effects models are emerging research areas in forestry (Calegario et al. 2005), but their applications in forest fire research are rarely reported. Studies of forest fires, based on multi-level aspects, such as combustible characteristics, fire forecasting and fire behavior, should reflect both overall change trend and individual differences, so NLME has more advantages (Guillermo et al. 2006). NLME also has the advantages of high reliability, flexibility and accuracy (Sharma et al. 2016), and have great application potential in the study of forest fire.

Declarations

Conflicts of interest The authors declare no conflicts of interest.

References

- Achtemeier GL (2006) Measurements of moisture in smoldering smoke and implications for fog. *Int J Wildland Fire* 15:517–525
- Akaike H (1974) A new look at the statistical model identification. *Trans Autom Control* 19:716–723
- Ballhom U, Siegert F, Mason M, Limin S (2009) Derivation of burn scar depths and estimation of carbon emissions with LIDAR in Indonesian peatlands. *Proc Natl Acad Sci USA* 106:21213–21218
- Bar-Ilan A, Rein G, Fernandez-Pello AC, Torero JL, Urban DL (2004) Forced forward smoldering experiments in microgravity. *Exp Thermal Fluid Sci* 28:743–751
- Bem PD, Osmar ACJ, Matricardi E, Guimarães RF, Gomes RAT (2018) Predicting wildfire vulnerability using logistic regression and artificial neural networks: a case study in Brazil. *Int J Wildland Fire* 28:35–45
- Budhathoki CB, Lynch TB, Guldin JM (2008) Nonlinear mixed modeling of basal area growth for shortleaf pine. *For Ecol Manag* 255:3440–3446
- Calama R, Montero G (2004) Interregional nonlinear height-diameter model with random coefficients for stone pine in Spain. *Can J For Res* 34:150–163
- Calegario N, Daniels RF, Maestri R, Neiva R (2005) Modeling dominant height growth based on nonlinear mixed-effects model: a clonal eucalyptus plantation case study. *For Ecol Manag* 204:11–21
- Cancellieri D, Leroy-Cancellieri V, Leoni E, Simeoni A, Kuzin AY, Filkov AI, Rein G (2012) Kinetic investigation on the smouldering combustion of boreal peat. *Fuel* 93:479–485
- Ciceu A, Garcia-Duro J, Seceleanu I, Badea O (2020) A generalized nonlinear mixed-effects height-diameter model for Norway spruce in mixed-uneven aged stands. *For Ecol Manag* 477:118507
- Davies GM (2016) Vegetation structure and fire weather influence variation in burn severity and fuel consumption during peatland wildfires. *Biogeosciences* 13:389–398
- Davies GM, Gray A, Rein G, Legg CJ (2013) Peat consumption and carbon loss due to smouldering wildfire in a temperate peatland. *For Ecol Manag* 308:169–177
- Dorado FC, Diéguez-Aranda U, Anta BM, Rodríguez MS, Gadow K (2006) A generalized height-diameter model including random components for radiata pine plantations in northwestern Spain. *For Ecol Manag* 229:202–213
- Hadden RM, Rein G, Belcher CM (2013) Study of the competing chemical reactions in the initiation and spread of smouldering combustion in peat. *Proc Combust Inst* 34:2547–2553
- Hall DB, Bailey RL (2001) Modeling and prediction of forest growth variables based on multilevel nonlinear mixed models. *For Sci* 47:311–321
- Hang LZ (1997) Cross-validation of non-Linear growth functions for modeling tree height-diameter relationships. *Ann Bot* 79:251–257
- Hartford R, Frandsen W (1992) When it's hot, it's hot or maybe it's not! surface flaming may not portend extensive soil heating. *Int J Wildland Fire* 2:139–144
- Hu Y, Fernandez-Anez N, Smith TEL, Rein G (2018) Review of emissions from smouldering peat fires and their contribution to regional haze episodes. *Int J Wildland Fire* 27:293–312
- Huang X, Rein G (2014) Smouldering combustion of peat in wildfires: inverse modelling of the drying and the thermal and oxidative decomposition kinetics. *Combust Flame* 161:1633–1644
- Huang X, Rein G (2017) Downward spread of smouldering peat fire: the role of moisture, density and oxygen supply. *Int J Wildland Fire* 26:907–918
- Huang X, Rein G, Chen H (2015) computational smoldering combustion: predicting the roles of moisture and inert contents in peat wildfires. *Proc Combust Inst* 35:2673–2681
- Huang X, Restuccia F, Gramola M, Rein G (2016) Experimental study of the formation and collapse of an overhang in the lateral spread of smoldering peat fires. *Combust Flame* 168:393–402
- Kalle E (2009) A multivariate linear mixed-effects model for the generalization of sample tree heights and crown ratios in the Finnish national forest inventory. *For Sci* 55:480–493
- Kirschke S, Bousquet P, Ciais P, Saunois M, Zeng G (2013) Three decades of global methane sources and sinks. *Nat Geosci* 6:813–823
- Kuhry P (1994) The role of fire in the development of sphagnum-dominated peatlands in western boreal Canada. *J Ecol* 82:899–910
- Leites LP, Robinson AP (2004) Improving taper equations of loblolly pine with crown dimensions in a mixed-effects modeling framework. *For Sci* 50:204–212
- Li C, Zhang H (2010) Modeling dominant height for Chinese fir plantation using a nonlinear mixed-effects modeling approach. *Scientia Silvae Sinicae* 46:89–95
- Lin S, Sun P, Huang X (2019) Can peat soil support a flaming wildfire? *Int J Wildland Fire* 28:601–613

- Mehtatalo L, Peltola H, Kilpelainen A, Ikonen VP (2014) The response of basal area growth of scots pine to thinning: a longitudinal analysis of tree-specific series using a nonlinear mixed-effects model. *For Sci* 60:636–644
- Meng S, Huang S (2009) Improved calibration of nonlinear mixed-effects models demonstrated on a height growth function. *For Sci* 55:238–248
- Mensah S, Pienaar OL, Kunneke A, Toit S, Seydack A, Uhl E, Pretzsch H, Seifert T (2018) Height-diameter allometry in south Africa's indigenous high forests: assessing generic models' performance and function forms. *For Ecol Manag* 410:1–11
- Nadeem K, Taylor SW, Woolford DG, Dean CB (2020) Mesoscale spatiotemporal predictive models of daily human- and lightning-caused wildland fire occurrence in British Columbia. *Int J Wildland Fire* 29:11–27
- Ohlemiller TJ (1985) Modeling of smoldering combustion propagation. *Prog Energy Combust Sci* 11:277–310
- Page SE, Siegert F, Rieley JO, Boehm HDV, Jaya A, Limin S (2002) The amount of carbon released from peat and forest fires in Indonesia during 1997. *Nature* 420:61–65
- Page SE, Rieley JO, Banks CJ (2011) Global and regional importance of the tropical peatland carbon pool. *Glob Change Biol* 17:798–818
- Pan L, Mei G, Wang Y, Saeed S, Chen L, Cao Y, Sun Y (2020) Generalized nonlinear mixed-effect model of individual tree height to crown base for *Larix olgensis* Henry in Northeast China. *J Sustain For* 39:1–14
- Pastor E, Oliveras I, Urquiagaflores E, Quintanoloayza JA, Mant MI, Planas E (2018) A new method for performing smoldering combustion field experiments in peatlands and rich-organic soils. *Int J Wildland Fire* 26:1040–1052
- Reardon J, Hungerford R, Ryan K (2007) Factors affecting sustained smoldering in organic soils from pocosin and pond pine woodland wetlands. *Int J Wildland Fire* 16:107–118
- Rein G, Cleaver N, Ashton C, Pironi P, Torero JL (2008a) The severity of smoldering peat fires and damage to the forest soil. *Catena* 74:304–309
- Rein G, Garcia J, Simeoni A, Tihay V, Ferrat L (2008b) Smoldering natural fires: comparison of burning dynamics in boreal peat and mediterranean humus. *Model Monit Manag For Fires* 119:183–192
- Rein G (2013) Smoldering fires and natural fuels. In: Belcher Claire M (ed) *Fire phenomena and the earth system: an interdisciplinary guide to fire science*. Wiley, Oxford
- Restuccia F, Huang X, Rein G (2017) Self-ignition of natural fuels: can wildfires of carbon-rich soil start by self-heating? *Fire Saf J* 91:828–834
- Rijal B, Weiskittel A, Kershaw JA (2012) Development of regional height to diameter equations for 15 tree species in the North American Acadian region. *Forestry* 85:379–390
- Sharma RP, Vacek Z, Vacek S (2016) Individual tree crown width models for Norway spruce and European beech in Czech Republic. *For Ecol Manag* 366:208–220
- Sheiner LB, Beal SL (1980) Evaluation of methods for estimating population pharmacokinetic parameters. I. michaelis-menten model: routine clinical pharmacokinetic data. *J Pharmacokin Biopharm* 8:553–571
- Shetler G, Turetsky MR, Kane E, Kasischke E (2008) Sphagnum mosses limit total carbon consumption during fire in Alaskan black spruce forests. *Can J for Res* 38:2328–2336
- Sinclair AL, Graham LLB, Putra EI, Saharjo BH, Applegate G, Grover SP, Cochrane MA (2020) Effects of distance from canal and degradation history on peat bulk density in a degraded tropical peatland. *Sci Total Environ* 699:134199
- Tang SY, Yin SN, Shan YL, Gao B, Sun L, Han XY, Wang MX, Wang MY, Chen ZS (2022) A study of emissions and marker gases from smoldering combustion in *Larix gmelinii* plantations of the Daxing'an Mountains. *J For Res* 33:195–201. <https://doi.org/10.1007/s11676-021-01323-x>
- Turetsky MR, Amiro BD, Bosch E, Bhatti JS (2004) Historical burn area in western Canadian peatlands and its relationship to fire weather indices. *Global Biogeochem Cycles* 18:1–9
- Turetsky MR, Benscoter B, Page S, Rein G, Guido RW, Watts A (2015) Global vulnerability of peatlands to fire and carbon loss. *Nature Geoscience* 8:11–14
- Wang S, Huang X, Chen H, Liu N (2017) Interaction between flaming and smoldering in hot-particle ignition of forest fuels and effects of moisture and wind. *Int J Wildland Fire* 26:71–81
- Watts AC, Kobziar LN (2013) Smoldering combustion and ground fires: ecological effects and multi-scale significance. *Fire Ecol* 9:124–132
- Yang Y, Huang S, Meng SX (2009) Development of a tree-specific stem profile model for white spruce: a nonlinear mixed model approach with a generalized covariance structure. *Forestry* 82:541–555
- Zaccone C, Rein G, Dorazio V, Hadden RM, Belcher CM, Miano TM (2014) Smoldering fire signatures in peat and their implications for palaeoenvironmental reconstructions. *Geochim Cosmochim Acta* 137:134–146

Publisher's Note Springer Nature remains neutral with regard to jurisdictional claims in published maps and institutional affiliations.